

Nonvolatile organic field-effect transistor memory element with a polymeric gate electret

Th. B. Singh,^{a)} N. Marjanović, G. J. Matt, and N. S. Sariciftci

Linz Institute for Organic Solar Cells (LIOS), Physical Chemistry, Johannes Kepler University Linz, Austria

R. Schwödauer and S. Bauer

Soft Matter Physics, Johannes Kepler University Linz, Austria

(Received 29 July 2004; accepted 1 October 2004)

Organic field-effect transistors with a polymeric electret as gate insulator and fullerenes as a molecular semiconductor were fabricated. We observed an amplification of the drain–source current I_{ds} on the order of 10^4 upon applying a gate voltage V_g . Reversing the gate voltage V_g features large metastable hysteresis in the transfer characteristics $I_{ds}(V_g)$ with a long retention time. The observation of a switchable channel current I_{ds} is proposed to originate from charge storage in the organic electret. As such, this device is a demonstration of an organic nonvolatile memory element switchable with the gate voltage. © 2004 American Institute of Physics. [DOI: 10.1063/1.1828236]

A nonvolatile memory device has a structure of a metal-oxide-semiconductor field-effect transistor (MOSFET) in which the conventional gate electrode is modified in a way to enable temporary charge storage inside the gate.¹ The time when the stored charge decreases to 50% of its initial value is defined as retention time. A long retention time is required for nonvolatile memory devices. Using inorganic semiconductors like Si, this has been used in integrated circuits since the last four decades.² Typically, there are two types of nonvolatile memory devices: floating gate devices and metal-insulator-oxide-semiconductor devices. Recently, insulators based on ferroelectric materials were utilized to fabricate nonvolatile memory devices.³

In organic electronics, much progress has been made in recent years in the development of FET based on organic semiconductors (OFET).⁴ There is much interest in research on OFETs with high mobility (μ) utilizing the large field of materials chemistry.⁵ Although the highest mobilities reported in *n*-channel OFETs (10^{-2} – 10^{-1} cm²/V s)⁴ are still lower than their inorganic counterparts, applications using low-cost production and large-area coverage such as radio-frequency IDs, smart tags, textile integrated electronics, etc., OFET devices and “plastic chips” are very attractive.⁶ Semiconducting plastics present particular advantages of plastic processing together with semiconductor properties. Solution-processed, large-area printable OFETs have quite some potential in future applications. In this sector, we want to explore a printable memory element with a polymeric electret as a gate dielectric for nonvolatile memory devices.

Dodabalapur *et al.* have made an attempt to realize an OFET with polarizable gate insulator which produces floating gate-like effects.⁷ A mechanism for the shift of the threshold voltage V_t (which is defined as gate voltage V_g where the free charge carrier density equals the trap density⁴) after applying a depleting V_g was proposed. Field-effect studies of OFETs with chemically modified gate dielectrics have observed a shift in V_t due to bias stressing.⁸ Hysteresis in the repeated capacitance–voltage measurements in different sweep directions of metal-oxide-organic-semiconductor

capacitor was demonstrated.⁹ Memory effect on OFETs with an inorganic ferroelectric and an organic semiconductor, namely, sexithiophene ($\alpha 6T$), was reported.¹⁰ Recently, OFETs based on organic “ferroelectric-like” insulators and pentacene were demonstrated.^{11–13} Evidence on the presence of trapping states at the insulator/organic semiconductor interface was also reported.¹⁴ However, an OFET based nonvolatile memory elements with an electret as gate insulator with a large V_g hysteresis and long retention time has not been realized as yet.

In this letter, we report results on detailed studies of an *n*-channel OFET using fullerenes in combination with a polymeric electret as the gate insulator. A large hysteresis for the source–drain current upon variation of the gate voltage is observed. This metastable effect is presumed to be due to charge storage and polarization within the bulk of the gate dielectric and/or at the interface between the electret and semiconductor.

The device fabrication starts with the etching of the indium tin oxide (ITO) on the glass substrate. After patterning the ITO and cleaning in the ultrasonic bath, polyvinyl alcohol (PVA) as a soluble electret was spin cast. PVA with a molecular weight of 100 000 was used, as received from Fluka Chemicals. The PVA was dissolved in distilled water and filtered using 0.2 μ m filters and lyophilized and redissolved again in distilled water. A 10 wt % ratio of a highly viscous PVA solution gives a film thickness of 0.6 to 1 μ m by spin coating at 1500 rpm. A methanofullerene [6,6]-phenyl C₆₁-butyric acid methyl ester (PCBM) active layer of 150 nm was spin coated on top of the PVA film from chlorobenzene solution (3 wt %) in argon atmosphere inside the glove box. The top source and drain electrode, Cr (20 nm), was evaporated under vacuum (3×10^{-6} mbar) through a shadow mask. All electrical characterization was carried out under an inert argon environment inside the glove box system. Keithley 236 and Keithley 2400 instruments were used for the steady state current–voltage measurements. Surface morphology and thickness of the dielectric and PCBM film were determined with a Digital Instrument 3100 atomic force microscope (AFM) and a Dektak surface profilometer.

A typical OFET structure is shown in Fig. 1 together with the chemical structure of the PVA and PCBM. The

^{a)}Electronic mail: birendra.singh@jku.at

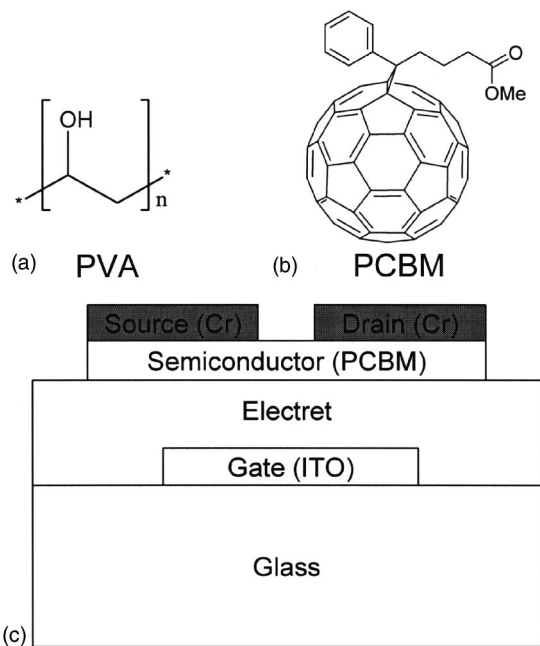


FIG. 1. Chemical structure of (a) PVA and (b) methanofullerene (PCBM). (c) schematic of the staggered mode nonvolatile memory OFET.

channel length L of the OFET is $65 \mu\text{m}$ and the channel width $W=1.4 \text{ mm}$. For the electret a thickness $d=1.4 \mu\text{m}$, dielectric constant, $\epsilon_{\text{PVA}}=5$ and capacitance of $C_{\text{PVA}}=3 \text{ nF/cm}^2$ were measured. This results a d/L ratio ≈ 0.02 , which is acceptable in order to avoid having the gate field screened by the source–drain contacts. Cr as a source–drain electrode is chosen because Cr does not significantly diffuse into the organic semiconductor layer.

The transistor characteristics $I_{\text{ds}}(V_{\text{ds}})$ is shown in Fig. 2 featuring an n -channel FET^{15–17} with electron accumulation mode with applied positive V_g and electron depletion mode with increasing negative V_g . A saturation of I_{ds} with increasing V_{ds} is obtained even when no V_g is applied. It is not yet clear as yet why FETs based on fullerenes have this “on” behavior with $V_g=0 \text{ V}$. The substrate surface may play a critical role in this effect; devices with substrates treated with amines have also been found to be “on,” as herein (Fig. 2).¹⁸

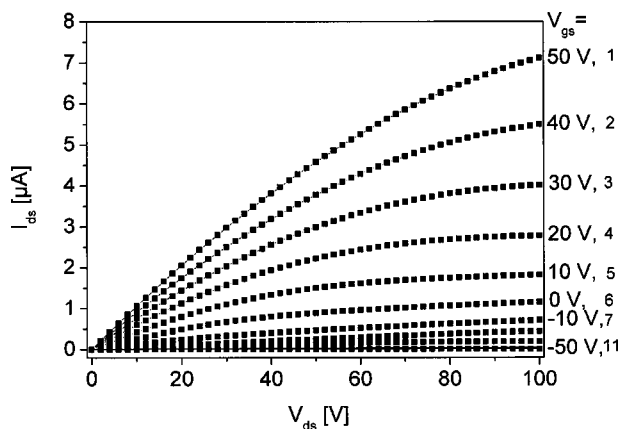


FIG. 2. Transistor characteristics of an OFET with channel length $L=65 \mu\text{m}$, channel width $W=1.4 \text{ mm}$ for different V_g . All measurements were carried out at room temperature. The data shown here are taken in descending V_g mode from 50 to -50 V in steps of 10 V as labeled from 1 to 11. The integration time is 1 s.

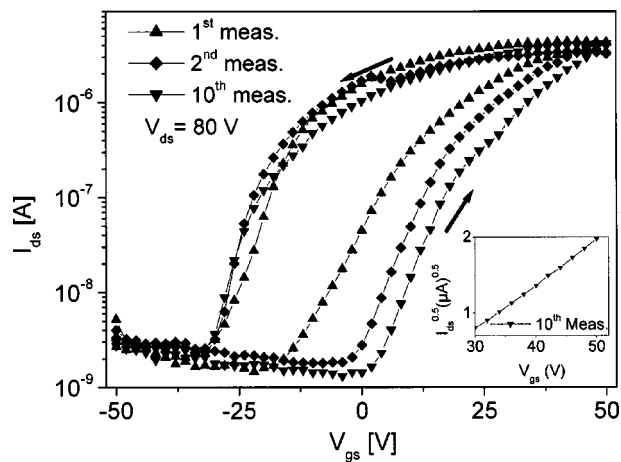


FIG. 3. Transfer characteristics of the OFET with $V_{\text{ds}}=80 \text{ V}$ demonstrating the nonvolatile organic memory device. Each measurement was carried out with an integration time of 1 s. Inset: $I_{\text{ds}}^{0.5}$ vs V_{gs} plot for the tenth measurement.

OFETs based on polycrystalline, evaporated C_{60} films show similar behavior.¹⁹

We observed a difference in $I_{\text{ds}}(V_{\text{ds}})$ plots while taking the data by increasing and/or decreasing the gate voltages. Data presented here are recorded when the gate voltage is applied in descending mode with 1 s integration time. The sequence of the measurement in Fig. 2 is labeled from 1 to 11. Transistor characteristics of the devices shows amplification factors up to 10^4 with the gate on/off.

The large hysteresis observed in V_g is shown in the transfer characteristics (I_{ds} versus V_{gs}) cycling the gate voltage (Fig. 3). All the OFET devices reported herein show a sharp turn-on voltage V_{to} , a voltage that is the x -intercept of the plot of $\sqrt{I_{\text{ds}}}$ versus V_g . Initial cycles feature a negative V_{to} , which develops into a stable hysteresis after few cycles, with a quadratic turn-on around 0 V . This allows us to calculate the mobility μ from the $\sqrt{I_{\text{ds}}}$ versus V_g plot, as shown in the inset of Fig. 3. A value of $\mu=9 \times 10^{-2} \text{ cm}^2/\text{V s}$ is obtained using Eq. (1):²

$$I_{\text{ds}} = \frac{\mu W C_{\text{PVA}}}{2L} (V_g - V_t)^2. \quad (1)$$

A μ of around $10^{-1} \text{ cm}^2/\text{V s}$ is relatively high as compared to the reports on PCBM devices using space charge limited currents^{20,21} and field-effect studies.²² The origin of this improved mobility here is proposed to be the homogeneous film formation on top of the smooth electret PVA with improved intermolecular transfer integral. We did not observe any significant dependence of this mobility upon variation of the source–drain metal electrodes like calcium and LiF/aluminium.

As presented in Fig. 3, the magnitude of the source–drain current I_{ds} increases with an amplification of up to 10^4 at $V_g \approx 50 \text{ V}$ with respect to the initial “off” state with $V_g=0 \text{ V}$. However, the saturated I_{ds} remain at high values even when V_g reduces back to $V_g=0 \text{ V}$. In order to completely deplete I_{ds} , one needs to apply a reverse voltage of $V_g \approx -30 \text{ V}$. A large shift in V_t by 14 V is observed when measured for the second time with respect to the initial cycle. Compared to the second measurement, the tenth measurement did not show a significant shift in V_t . Each measurement was performed with a long integration time of 1 s with

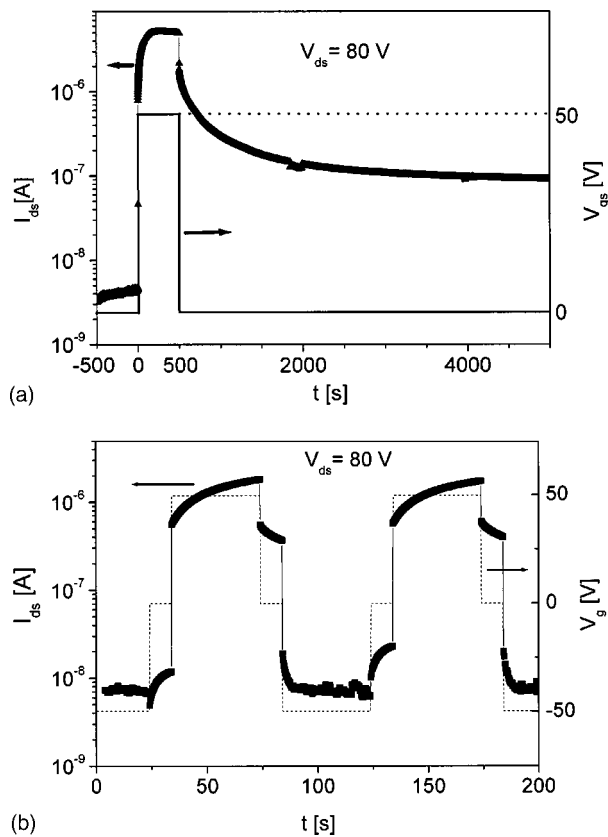


FIG. 4. (a) Logarithmic I_{ds} vs time (t) plot at $V_{ds}=80$ V for floating gate (denoted by $V_g=0$ V), during $V_g=50$ V and floating gate sequentially showing long retention time. The data were taken each 250 ms and every second data point is plotted. (b) Switching response of the drain current, upon application of gate voltage pulses with a pulse height of ± 50 V and a pulse duration of 40 s.

a step voltage of 2 V. Our result indicates that there is minimal gate bias stress in these devices.⁸ This observation is proposed to be due to locally trapped charges that induce shifts in V_t .

To estimate the retention time of the stored charges remaining in the electret (i.e., storage time of the memory element), time-resolved measurements were performed [Figs. 4(a) and 4(b)]. First, the device was biased with $V_{ds}=80$ V and kept at floating gate. At time $t=0$ s, $V_g=50$ V is applied until a stable current is obtained. After a time $t=500$ s the device is again in floating gate mode. I_{ds} remains high (memory “on” state) for more than 15 h. This implies that once the electret is charged fully, the relaxation of the charges is a slow process, as expected for charged electrets.²³ No detectable degradation has been observed after this long measurement time. In Fig. 4(b) the write/read/erase/read cycles are demonstrated with write/erase pulses using positive and negative gate voltages, respectively. The read of the memory state is done by monitoring the I_{ds} . High I_{ds} denotes “on” and low I_{ds} denotes the “off” state of the memory unit. The device presents a quite long response time due to the electret mechanism of charge storage, as discussed subsequently, but improvements seem possible with thinner gate dielectrics.

Our results cannot be explained by a dipole polarization mechanism of the electret,⁷ since capacitance voltage measurement showed a negligible hysteresis. Therefore, trapping of the injected charges is proposed. Further measurements of

the temperature-dependent transfer characteristics $I_{ds}(V_{gs})$ are also in favor of the charge trapping mechanism.¹⁹ However, a detailed study is required to locate the trapped charges. Charging and discharging of PVA films is well known,²⁴ and significant charge trapping in PVA-based polymers was also reported by others.²⁵

In conclusion, we demonstrated an organic nonvolatile memory device based on OFETs using a polymeric electret as gate dielectric. The results indicate the metastable charging of the electret with an applied gate voltage resulting in very long retention times up to hours.

This work was performed within the Christian Doppler Society’s dedicated laboratory on Plastic Solar Cells funded by the Christian Doppler Society and Konarka Austria GesmbH.

¹*Nanoelectronics and Information Technology: Advanced Electronic Materials and Novel Devices*, edited by R. Waser (Wiley-VCH, Weinheim, 2003).

²D. Kahng and S. M. Sze, *Bell Syst. Tech. J.* **46**, 1283 (1967); S. M. Sze, *Physics of Semiconductor Devices* (Wiley, New York, 1981), p. 496.

³S. Mathews, R. Ramesh, T. Venkatesan, and J. Benedetto, *Science* **276**, 138 (1997).

⁴C. D. Dimitrakopoulos and D. J. Maseo, *IBM J. Res. Dev.* **45**, 11 (2001); G. Horowitz, *Adv. Funct. Mater.* **13**, 53 (2003).

⁵V. Podzorov, S. E. Sysoev, E. Loginova, V. M. Pudalov, and M. E. Gershenson, *Appl. Phys. Lett.* **83**, 3504 (2003).

⁶J. A. Rogers, Z. Bao, K. Baldwin, A. Dodabalapur, B. Crone, V. R. Raju, V. Kuck, H. Katz, K. Amundson, J. Ewing, and P. Drzaic, *Proc. Natl. Acad. Sci. U.S.A.* **98**, 4835 (2001).

⁷H. E. Katz, X. M. Hong, A. Dodabalapur, and R. Sarpeshkar, *J. Appl. Phys.* **91**, 1572 (2002).

⁸A. Salleo, M. L. Chabinyk, M. S. Yang, and R. A. Street, *Appl. Phys. Lett.* **81**, 4383 (2002).

⁹S. Scheinert, G. Paaasch, S. Pohlmann, H.-H. Horhold, and R. Stockmann, *Solid-State Electron.* **44**, 845 (2000).

¹⁰G. Velu, C. Legrand, O. Tharaud, A. Chapoton, D. Remiens, and G. Horowitz, *Appl. Phys. Lett.* **79**, 659 (2001).

¹¹R. Schroeder, L. A. Majewski, and M. Grell, *Adv. Mater. (Weinheim, Ger.)* **16**, 633 (2004).

¹²T. Kotzasa, M. Yoshida, S. Uemura, and T. Kamata, *Synth. Met.* **137**, 943 (2003).

¹³K. N. N. Unni, R. de Bettignies, S. Dabos-Seignon, and J. M. Nunzi, *Proc. SPIE* **5351**, 166 (2004).

¹⁴L. Torres, D. M. Taylor, and E. Itoh, *Appl. Phys. Lett.* **85**, 314 (2004).

¹⁵T. Kanbara, K. Shibata, S. Fujiki, Y. Kubozono, S. Kashino, Y. Kubozono, S. Kashino, T. Urishi, M. Sakai, A. Fujiwara, R. Kumashiro, and K. Tanigaki, *Chem. Phys. Lett.* **379**, 223 (2003).

¹⁶S. Kaboyashi, S. Mori, S. Lida, H. Ando, T. Takenobu, Y. Taguchi, A. Fujiwara, A. Taninaka, H. Shinohara, and Y. Iwasa, *J. Am. Chem. Soc.* **125**, 8116 (2003).

¹⁷K. Shibata, Y. Kubozono, T. Kanbara, T. Hosokawa, T. Hosokawa, A. Fujiwara, Y. Ito, and H. Shinohara, *Appl. Phys. Lett.* **84**, 2572 (2004).

¹⁸R. C. Hoddon, A. S. Perel, R. C. Morris, T. T. M. Palstra, A. F. Hebard, and R. M. Fleming, *Appl. Phys. Lett.* **67**, 121 (1995).

¹⁹Th. B. Singh, N. Marjanović, G. J. Matt, S. Gunes, N. S. Sariciftci, R. Schwödau, S. Bauer, A. Andreev, A. Montaigne, and H. Sitter (unpublished).

²⁰V. D. Mihailtchi, J. K. J. van Duren, P. W. M. Blom, J. C. Hummelen, R. A. J. Janssen, J. M. Kroon, M. T. Rispens, W. J. H. Verhees, and M. M. Wienk, *Adv. Funct. Mater.* **13**, 43 (2003).

²¹G. J. Matt, N. S. Sariciftci, and T. Fromherz, *Appl. Phys. Lett.* **84**, 1570 (2004).

²²C. Waldauf, P. Schilinsky, M. Perisutti, J. Hauch, and C. J. Brabec, *Adv. Mater. (Weinheim, Ger.)* **15**, 2084 (2003).

²³R. Gerhard-Mulhaupt and G. Sessler, *Electrets* (Laplacian, Morgan Hill, 1999), Vol. I and II.

²⁴K. Lakshminarayana, Y. Dasaradhu, and V. V. R. N. Rao, *Mater. Lett.* **21**, 425 (1994).

²⁵P. Frübing, M. Wegener, R. Gerhard-Mulhaupt, A. Buchsteiner, W. Neumann, and L. Brehmer, *Polymer* **40**, 3413 (1999).